Hindawi
Advances in Meteorology
Volume 2018, Article ID 2512138, 14 pages
https://doi.org/10.1155/2018/2512138

Research Article

A Persistent Fog Event Involving Heavy Pollutants in Yancheng Area of Jiangsu Province

Yuying Zhu[1,2], **Chengying Zhu**[1,2], **Fan Zu**[1,2], **Hongbin Wang**[1,2], **Chengsong Yuan**[1,2], **Shengming Jiao**[1,2] **and Linyi Zhou**[1,2]

[1]*Key Laboratory of Transportation Meteorology, China Meteorological Administration, Nanjing 210009, China*
[2]*Jiangsu Institute of Meteorological Sciences, Nanjing 210009, China*

Correspondence should be addressed to Hongbin Wang; kaihren@163.com and Chengsong Yuan; 41235772@qq.com

Received 19 December 2017; Revised 27 March 2018; Accepted 24 April 2018; Published 5 June 2018

Academic Editor: Pedro Salvador

In the early December 2013, dense fog involving heavy pollutants lasted for 9 days in the Yancheng area. The characteristics, formation, and lasting mechanisms of this persistent fog were analyzed based on observational data at the Sheyang site, reanalysis data, and final analysis data from NCEP/NCAR, combining with the weather background and meteorological and physical variable fields. Results include that (1) the fog process was characterized by long duration, low visibility, and high pollutants concentration, (2) the atmospheric general circulation contributed to the sustainability and development of the heavily polluted fog, (3) deep inversion was the key thermal factor causing the heavily polluted fog, (4) the fog exhibited obvious outbreaks with good visibility weather turned to severe fog several times, and (5) the weak cold air invasion and radiative cooling were the triggering factors to the sudden enhancement of the fog.

1. Introduction

Fog is a phenomenon due to lots of water droplets or ice crystals suspended in the air of the ground layer, which makes horizontal visibility decline to 1 km or less [1]. Haze is a phenomenon due to the aggregation of lots of tiny dust particles, soot, or salt particles suspended in the air, which makes horizontal visibility decline to 10 km or less [2]. Fog limits the visibility and thus affects human activities that rely on good visibility conditions. These activities are part of the core activities of modern societies, most notably aircraft operations, shipping [3], and road traffic [4]. Moreover, when the fog contains heavy pollutants, it is also harmful to human health [5]. This is why accurate forecasts of fog and haze have become an important issue.

The observation [6, 7] and modelling [8, 9] of dense fog have been studied in recent years. Several dynamic, thermal, and water vapor conditions including the layered structure of thermal inversion, the increase of temperature in the ground layer after sunrise, and the vertical transmission of heat, momentum, and water vapor caused by turbulent mixing have been found that trigger to dense fog [1, 10, 11]. Severe fog in China was first reported in a study on the Shanghai-Nanjing expressway [12]. From then on, more field observations were launched in different seasons and regions in China [13–17]. Results from these studies showed that the longwave radiation enhancement at night, evaporation from the wet surface after sunrise, and turbulent mixing are three main physical factors on fog enhancement [18, 19]. Liu et al. [20] analyzed the boundary layer features of a persistent advection fog process in the Yangtze River delta region and found that the double-inversion structure provided good thermal conditions for the thick fog, and the southeast vapor transport was not only conducive to maintaining the thickness of the fog but also sustained its long duration. Ma et al. [21] studied a fog case in central and southern Hebei Province and reported that the maintenance of the northeasterly winds was the main reason promoting the heavy fog. A rarely seen heavy fog occurred in Jiangsu Province during 24–27 December 2006, and it lasted for 64 h in Nanjing, with severe fog taking place over 41 h [22].

Recently, many studies revealed that when severe fog formed, it usually showed obvious explosive features, including sudden surge of fog drop number density, obvious increase in the fog drop scale and water content, sharp plunge of visibility from several hundred meters to below 50 meters, and fast changing from heavy fog to severe fog within a very short time period (about 30 min) [23]. With the improvement of temporal resolution of droplet spectrometer, Li et al. [24] analyzed microphysics processes and macroscopic conditions of fog droplet spectrum widening. He pointed out that the former stage of fog droplet spectrum widening mainly involved nucleation and condensation processes, while the latter stage mainly involved coagulation and condensation processes. Turbulence not only plays a significant role in heat, momentum, and moisture vertical transfers but also is the necessary condition for coagulation and increase of fog droplet. Researchers analyzed chemical characteristics of fog through conducting field observations [25–29] and improved forecasting capability of fog models by parameterizing microphysics features of fog over the sea and land. They also explained fog droplet excitation and fog formation through analysis on turbulence mixing and observations. A number of studies revealed the phenomenon of fog droplet increasing [30–35], mainly due to the factors of supersaturation and radiative cooling. Choularton et al. [36] found that radiative cooling alone cannot produce large fog droplets, while greater supersaturation and turbulence can promote the formation of large droplets.

Although fog and haze are different weather phenomena, their formations have similarity. They all form under breeze, high humidity, and static stability condition. Many studies indicated that the two can convert from one to the other [37–39]. Köhler [40] suggested that the haze aerosols can be transformed to fog droplets under certain conditions. Hygroscopic aerosols can become haze droplet before the saturation reaches the critical supersaturation S_c, and when the environmental saturation is equal or larger than S_c, the aerosol particles can be activated spontaneously. Before fog occurs, it is frequently accompanied with haze or heavy haze for a certain time; and after the fog dissipates, the haze will appear [41].

Despite there were efforts focusing on thick fog and haze, basic research is still needed with respect to the explosive development of fog and interactions between dense fog and heavy pollutants. In the early December 2013, a continuous heavy fog which was rare in record in terms of long duration, low visibility, and heavy pollution appeared in Yancheng, Jiangsu Province, China. In this study, the formation and maintaining mechanisms of this dense fog with strong pollutants are comprehensively analyzed by using the observational data at the Sheyang site (120.15°E, 33.46°N), reanalysis data, and final analysis data from NCEP/NCAR. The aim of this study was to discuss the causes of heavy pollution and analyze reasons and mechanism of the fog's explosiveness, which would be helpful to our better understanding of fog-related processes and fog-forecasting issues.

The article is structured as follows: Section 2 describes the data used in this study and the classification of grade of fog and air quality, respectively. Section 3 shows the features of this fog event, including long duration, explosive enhancement, and heavy pollution. Section 4 is concerned with the weather conditions contributing to the maintenance of strongly polluted fog, while Section 5 presents the thermal and dynamic conditions. Section 6 focuses on the causes for the explosive development of severe fog, and in Section 7, results are summarized, and conclusions are drawn.

2. Site and Data

2.1. Observational Site and Data. The visibility of less than 0.2 km due to fog is defined as severe fog, and that of less than 0.05 km, extremely dense fog [42]. The air quality is classified as four categories: excellent, good, slightly polluted, and severe polluted. According to the standards by China Meteorological Administration (CMA), if the primary pollutant is $PM_{2.5}$ and the daily-averaged concentration exceeds 250 $\mu g \cdot m^{-3}$, it is considered as severely polluted [43].

The thick fog with heavy pollutants was observed from 1 to 9 December 2013 in Yancheng, Jiangsu Province, China. This weather phenomenon lasted for 9 days, with severe fog which occurred 6 times. The duration was about 35 min, 2 h, 25 min, 9 h, 5.5 h, and 7.3 h, respectively. Moreover, five of them developed into extremely dense fog, with explosive enhancement feature each time. Furthermore, pollution was particularly heavy, with the maximum of the $PM_{2.5}$ concentration reaching 764 $\mu g \cdot m^{-3}$. It was also recorded by a meteorological observatory. This kind of weather phenomenon had not been observed in the recent decades. The rarity justifies our discussion.

The observational datasets are from the Sheyang site (elevation 1.8 m, 120.15°E, 33.46°N) in Yancheng, which is located in the eastern part of the Jiangsu Province (Figure 1). The meteorological variables being observed include 10 m wind speed and direction, 2 m air temperature, and 2 m relative humidity, which are sampled every 10 min. The visibility is obtained every 1 min at 2 m height. The boundary layer is observed via the radiosonde. The balloon takes the sensor up at speed of 400 meters per minute and records temperature, pressure, humidity, wind direction, and wind speed information at different altitudes. The observations are taken twice a day, 07:00 Beijing Time (BT) and 19:00 BT. The concentrations of three major pollutants, including $PM_{2.5}$, SO_2, and NO_2 are also observed.

2.2. Reanalysis Data and Final Analysis Data. To represent the atmospheric circulation fields, the daily data of the National Centers for Environmental Prediction/National Center for Atmospheric Research (NCEP/NCAR) global reanalysis from 1 December 1979 to 31 December 2013 are utilized. Variables used here include geopotential height, temperature, and U-component and V-component of wind, with 17 levels. The horizontal resolution for the NCEP/NCAR reanalysis is $2.5° \times 2.5°$.

The final analysis data of NCEP/NCAR are used during the fog event from 1 to 9 December 2013, including variables

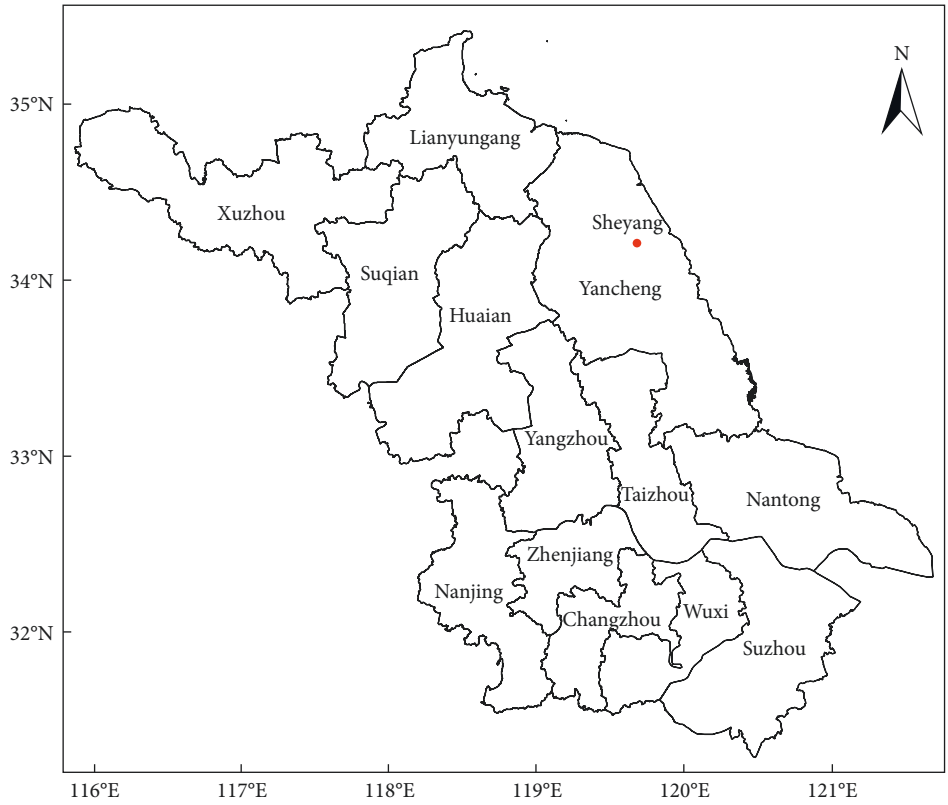

Figure 1: Map showing the location of the Sheyang site in Jiangsu Province.

of sea-level pressure, wind field at 10 m height, and U-component and V-component of wind with 17 levels. The horizontal resolution is $1^\circ \times 1^\circ$. The analysis data are taken four times a day: 02:00 BT, 08:00 BT, 14:00 BT, and 20:00 BT.

3. Fog Observation and Features

On the surface weather chart of 29-30 November 2013, Jiangsu Province was in front of a dry trough located over north China plain, with wind speed approximately 4–6 $m \cdot s^{-1}$, and depression of the dew point higher than 5°C. High-wind speed and dry air resulted in good visibility. During 1–9 December 2013, two high-pressure systems occurred from northern Xinjiang to west of Baikal Lake and from Northeast China to Southeast Russia, respectively. A low-pressure center appeared from Southwest China to Southeast Asian region, while Central and East China were under uniform pressure, with breeze or calm wind. Heavy fog and severe fog appeared successively in Jiangsu Province. Until 9 December, Mongolia high moved southward and eastward, and the cold air invaded, causing the fog to dissipate. The fog process was characterized by long duration, strong intensity, and heavy air pollution.

From 1 to 9 December, the Yancheng area was mostly foggy. During 1 December night, the sky was partly cloudy and the wind speed was 1 $m \cdot s^{-1}$. Due to radiative cooling, the fog began to form at about 23:00 BT. Extremely dense fog appeared at some sites in the southern Yancheng and expanded to northern Yancheng gradually. Until the early morning of 5 December, the extremely dense fog almost occupied the entire Yancheng area. What is worse was that as the fog turned into dense or even extremely dense fog, the air pollution also became severe. These dense fogs showed explosive development characteristics.

3.1. Long Duration. Long duration of severe fog was an important characteristic of this fog event. Figure 2 shows the temporal variation curves of visibility, relative humidity, temperature, wind direction, and speed at the Sheyang site. These curves reveal that since the morning of 2 December, the visibility at this station dropped sharply, and extremely dense fog appeared, which continued to 09:00 BT on 2 December. From 20:00 BT on 3 December to 02:00 BT on 4 December, some area in Yancheng had weak precipitation and thus supplied moisture for the fog development. When the sky cleared up, extremely dense fog appeared again. In the afternoon of 4 December, the visibility had improved; but at night, the fog broke out again and turned into an extremely dense one. In the afternoon of 5 December, the fog intensity weakened, and the visibility on 6 December remained above 1 km. From 00:00 BT to 08:00 BT on 7 December and from 18:00 BT on 8 December to 06:00 BT on 9 December, severe fog events occurred again and again. After 07:00 BT on 9 December, as cold air moved in, the visibility returned to 1 km or better. The whole fog event lasted for 9 days, and extremely dense fogs occurred frequently during the period, with the longest extremely dense fog lasting for as long as 9 hours.

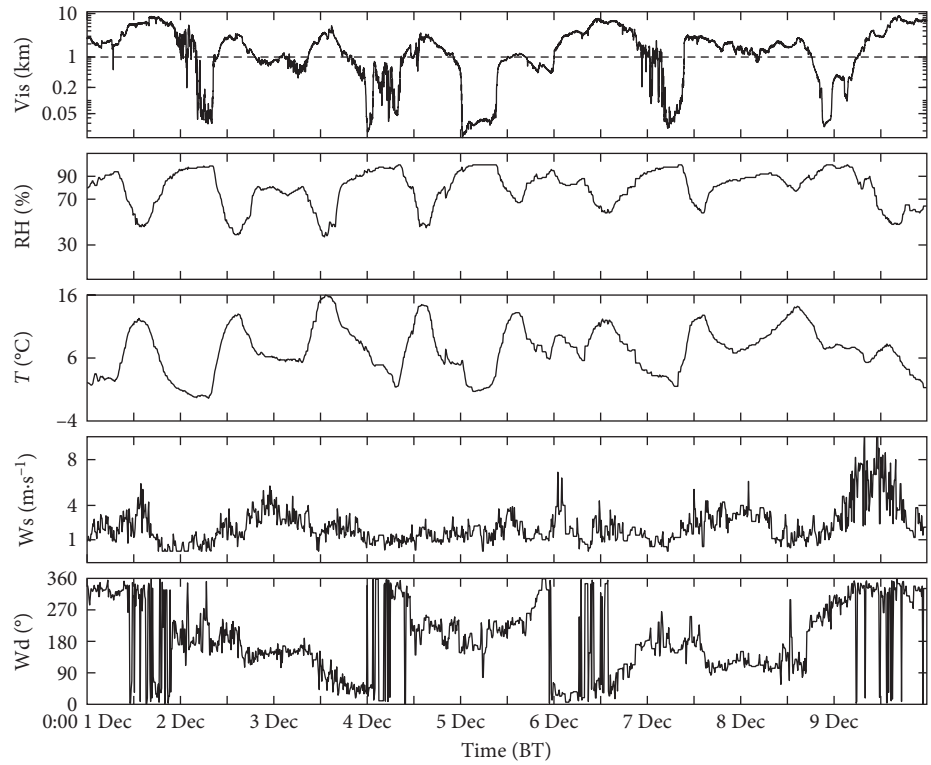

Figure 2: Temporal variation of visibility, relative humidity, temperature, wind speed, and wind direction at the Sheyang site from 1 to 9 December 2013.

3.2. Explosive Enhancement Characteristics. The characteristic of the formation of the dense fog in the Yancheng area was explosiveness, since the fog enhanced into severe fog or extremely dense fog within a very short time (about 30 min). This feature can be seen in the visibility variation curves of five fog cases recorded at the Sheyang site, which is shown in Figure 3. Table 1 lists the starting time, ending time, and the visibility of these five cases, indicating that explosive enhancement happened almost within 30 min and the shortest one was only 8 min. Another noticeable feature seen from Cases 1 and 4 is that light fog events with the visibility over 1 km turned into severe fog or extremely dense fog, which was rarely seen in previous observations. Figure 3 also shows that some fog processes had several explosive enhancements, such as Case 4 with four explosive enhancements, in which the second and third explosive enhancements burst into severe fogs again after the fog dissipated.

3.3. Heavy Pollution. This fog event in Yancheng had another important characteristic: heavy pollution. As the atmospheric stratification was stable and the inversion layer existed for a long time, a large amount of contaminated particles and polluted gases accumulated in the ground layer, causing heavy pollution. Figure 4 presents the hourly curves of $PM_{2.5}$ concentration and contaminated gases at the Yancheng site during 1–9 December. We can see that, on 2, 3, 5, and 9 December, the concentration of $PM_{2.5}$ was particularly high with an average value higher than 250 $\mu g \cdot m^{-3}$ that belongs to serious pollution category according to the CMA standard. In particular, at 21:00 BT on 4 December, the hourly concentration of $PM_{2.5}$ was up to 764 $\mu g \cdot m^{-3}$, about 1-2 times higher than the other fog or haze events reported [44, 45]. The situation was not improved until the midnight of 4 December, due to precipitation before the next fog occurrence. Thanks to the strong northwesterly winds, the fog began to dissipate on 9 December, and the $PM_{2.5}$ concentration dropped rapidly. Moreover, we may conclude that the dense fog and heavy pollution happened at the same time as a whole. Seriously polluted fog is not only harmful to human health but also has a strong extinction effect because of its hygroscopic property, which greatly reduces the visibility.

As is shown in Figure 4, the polluted gases generally began to rise after sunrise and reached their maximum concentrations during noon to dusk. The content of SO_2 reached a peak at 11:00 BT on 3 December, with the value of 142 $\mu g \cdot m^{-3}$, and the maximum content of NO_2 was 126 $\mu g \cdot m^{-3}$ at 18:00 BT on 2 December. Figure 4 also indicates that when the dense fog occurred, the polluted gases decreased obviously, which was significantly different from that of $PM_{2.5}$. Due to the large number of polluted gases dissolved in the fog, the polluted gases concentration decreased, which resulted in the increase of fog ion concentration and acidity [38, 41]. Previous research suggested that nitrate and sulfate are mostly contained in the noncoarse modes, with the conversion of NO_2 and SO_2 occurring mostly via gas-phase oxidation followed by condensation or through droplet mode sulfate produced from the fog process [46–48]. Shi et al. [41] found that the concentration of NO_3^- and SO_4^{2-} in foggy days are about 10 times and 2 times higher

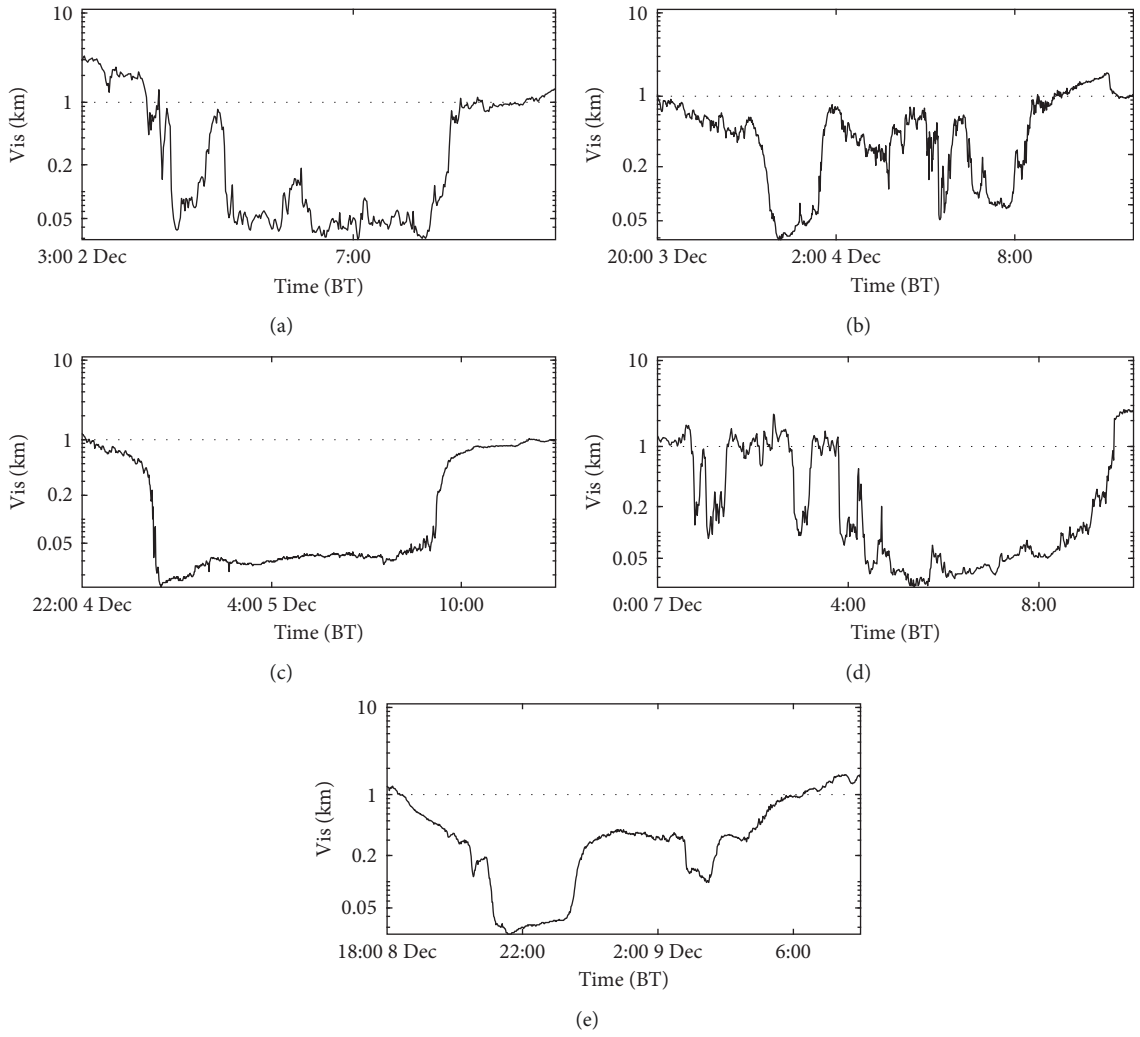

Figure 3: Temporal variation of visibility during five explosive processes at the Sheyang site. (a) Case 1: from 03:00 BT on 2 December to 10:00 BT on 2 December; (b) Case 2: from 20:00 BT on 3 December to 12:00 BT on 4 December; (c) Case 3: from 22:00 BT on 4 December to 13:00 BT on 5 December; (d) Case 4: from 00:00 BT on 7 December to 10:00 BT on 7 December; (e) Case 5: from 18:00 BT on 8 December to 08:00 BT on 9 December.

than those in clear days. This is the result of gas to particle phase conversion under fog conditions. In our study, the increase in $PM_{2.5}$ concentrations could be related to the formation of secondary aerosol in the atmosphere [49–51]. In addition, the strong inversion layer in the highly stable atmospheric condition is also a very important factor causing the high $PM_{2.5}$ concentrations.

4. Weather Condition Beneficial to the Maintenance of Strongly Polluted Fog

The severely polluted fog event lasted for 9 days, and the weather condition contributed to this event. Figure 5 shows the distributions of anomaly fields for geopotential height, temperature, wind speed, and wind field in the middle and lower troposphere in the early December 2013. In the lower troposphere (925 hPa), the air pressure over mainland China was lower, the anomalous westerly or southwesterly wind were located along the east coast in the South China Sea, the Malay Peninsula, and Indonesia, which indicated that the East Asian winter monsoon weakened at that time. Therefore, the southwesterly anomalies appeared in the lower troposphere in Jiangsu, with lower wind speed and higher temperature. In the middle troposphere (500 hPa), a significant positive height anomaly center was formed south of Lake Baikal (110°E, 50°N); meanwhile, a negative anomaly covered the area over (140°E, 27.5°N). Thus, the high-pressure center weakened, the corresponding surface circulation weakened, and the surface wind speed decreased. The East Asia trough enhanced, the cold air invasion strengthened, and the temperature in the middle troposphere became lower over Jiangsu Province, which was related to the frequent passages of the westerly trough. In addition, the area north of 30°N in East China was under easterly anomalies at 700 hPa, which was detrimental to the cold air invasion from the north and made the temperature higher at 700 hPa over Jiangsu Province. To reveal the vertical distribution characteristics of anomalous atmospheric background condition, Figure 6 shows the

Table 1: The beginning and ending times of five explosive processes and the visibility at each time.

	Time	Visibility (km)
Case 1		
Beginning	03:57 BT on 2 December	1.142
Ending	04:24 BT on 2 December	0.037
Case 2		
Beginning	23:11 BT on 3 December	0.517
Ending	23:47 BT on 3 December	0.042
Case 3		
Beginning	23:52 BT on 4 December	0.537
Ending	00:20 BT on 5 December	0.027
Case 4		
Beginning	00:36 BT on 7 December	1.772
Ending	01:04 BT on 7 December	0.085
Beginning	02:41 BT on 7 December	1.587
Ending	02:58 BT on 7 December	0.092
Beginning	03:47 BT on 7 December	1.29
Ending	03:55 BT on 7 December	0.071
Beginning	04:13 BT on 7 December	0.553
Ending	04:27 BT on 7 December	0.033
Case 5		
Beginning	20:18 BT on 8 December	0.298
Ending	21:08 BT on 8 December	0.04

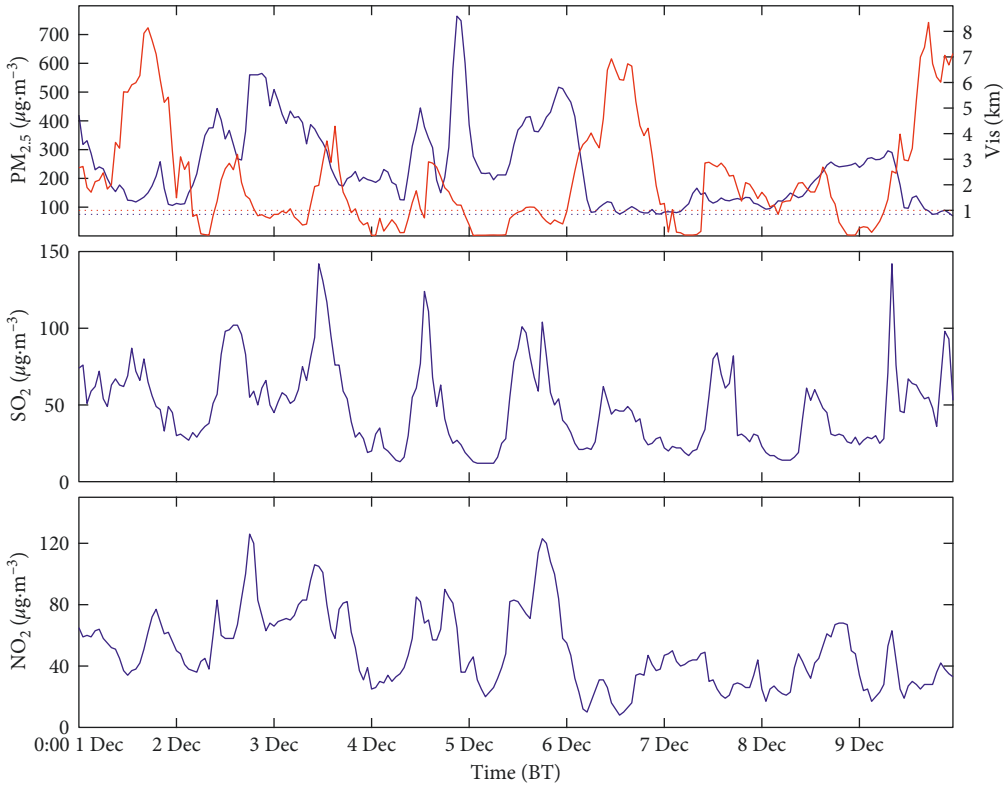

Figure 4: Time series of air pollutants concentration at the Yancheng site from 1 to 9 December 2013. The dotted red line represents 1 km visibility, and the dotted blue line represents 75 $\mu g \cdot m^{-3}$ $PM_{2.5}$ concentration.

anomalous variation of regionally averaged horizontal wind speed and regionally averaged temperature of Jiangsu Province (115–122.5°E, 30–35°N) with height. The horizontal wind speed weakened in the whole troposphere. In the middle and lower troposphere (850 hPa) and above the upper troposphere (200 hPa), the weakening of wind speed decreased with height. In the troposphere from 850 to 300 hPa, it was the opposite; that is, the weakening of wind speed increased with

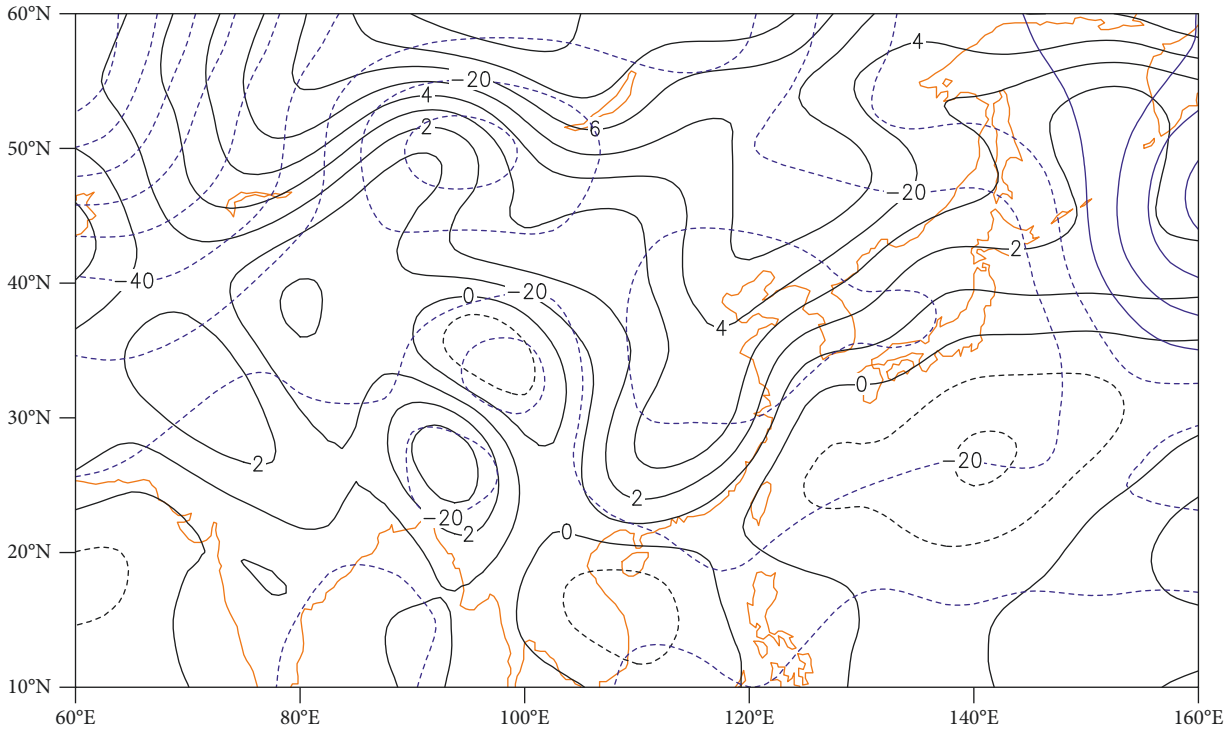

(a)

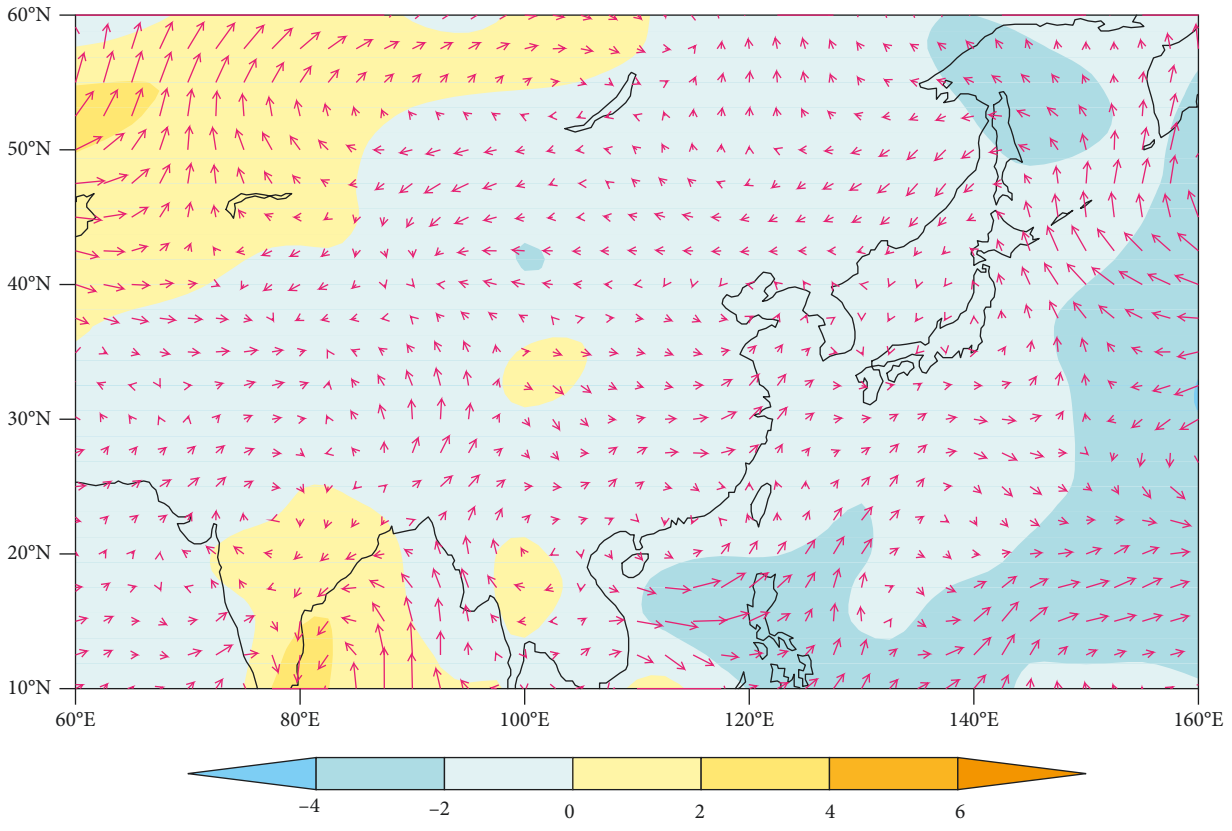

(b)

Figure 5: Continued.

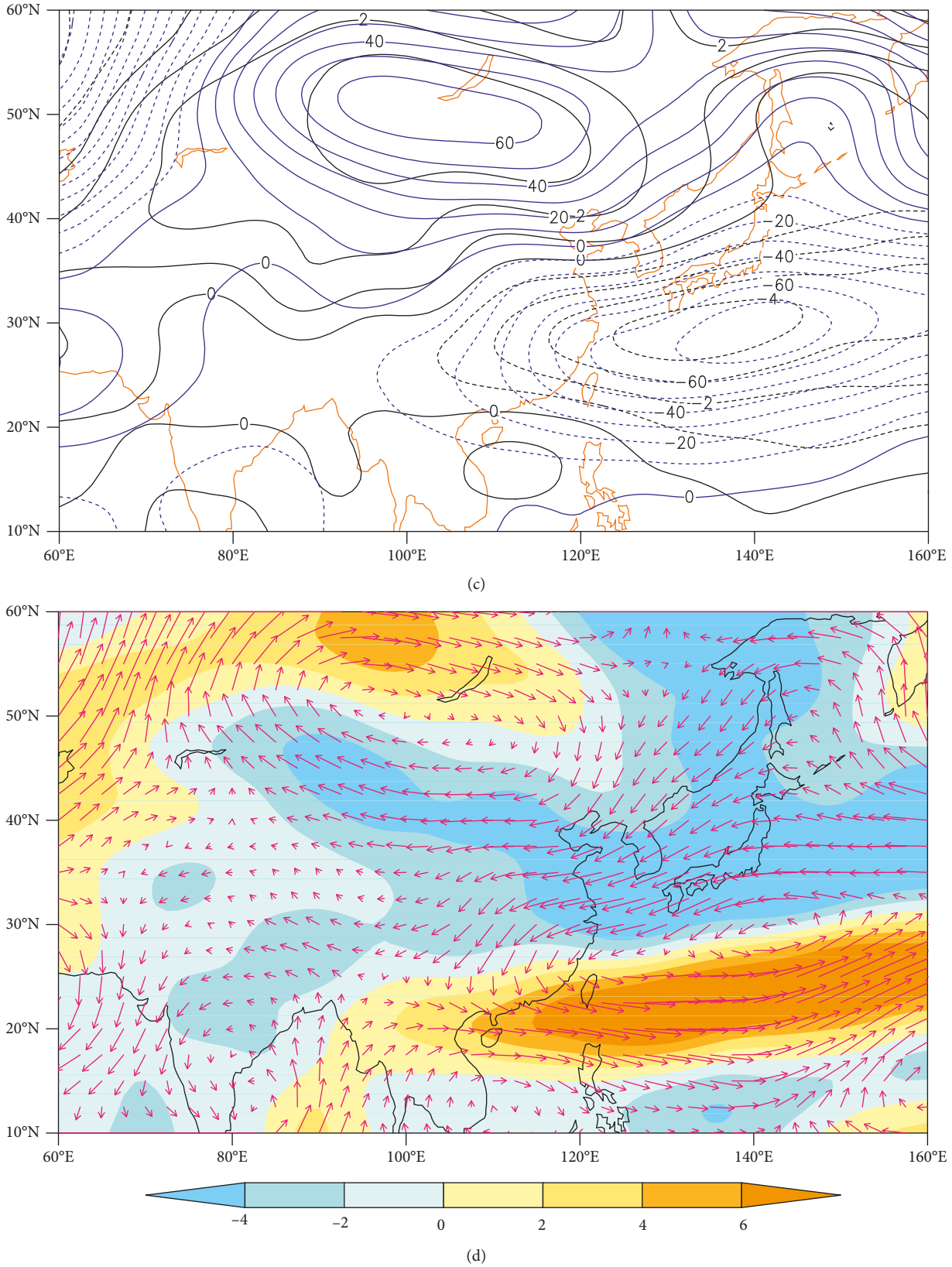

Figure 5: Spatial patterns of anomalous fields at 925 hPa from 1 to 9 December 2013. (a) Geopotential height and temperature. The blue contours are geopotential height (gpm), and the black contours are temperature (°C). (b) Wind speed and wind direction. The red arrows represent the wind direction (°), and the shading represents the wind speed ($m \cdot s^{-1}$). Subplots (c) and (d) are the same as subplots (a) and (b), respectively, but for anomalous fields at 500 hPa.

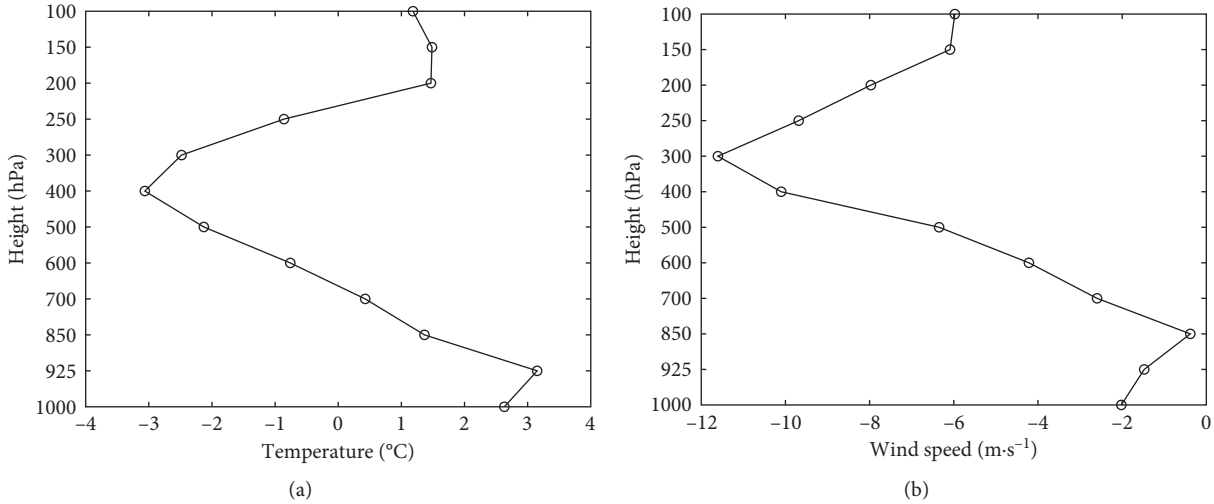

Figure 6: Vertical profiles of temperature anomaly (a) and wind speed anomaly (b) of Jiangsu area from 1 to 9 December 2013.

height. The distribution of regionally averaged temperature anomaly with height shows that the whole middle and lower troposphere (700 hPa) had uniform warming, while below 925 hPa, positive temperature anomaly increased with height, which indicated the presence of a thermal inversion layer.

Thus, the high-pressure control for a long time was the cause for the long-lasting polluted fog. Meanwhile, the southwesterly wind anomaly at the middle and lower troposphere was conductive to the transportation of moisture from South China to Jiangsu Province, which provided the moisture for the polluted fog. In addition, the thermal inversion layer in the lower troposphere made the atmosphere more stable and provided thermodynamic condition for the fog development. These atmospheric background conditions were all beneficial to the development and maintenance of the polluted fog.

5. Thermal and Dynamic Structures Beneficial to Maintaining the Strongly Polluted Fog

In the course of this fog event, why did the extremely dense fog with visibility below 50 m last for several days in succession, and why was the pollution so heavy? These are key issues that need to be researched.

Figure 7 shows the temperature and relative humidity profiles based on the radiosonde data at the Sheyang site. The thermal inversion structure was maintained both in the morning and in the evening during the entire fog event. The thickness of the inversion layer was between 100 and 700 m, and the average intensity was 3.5°C/100 m. During 2–5 December of the strongly polluted fog, the top of the inversion layer was under 200 m, and the intensity of inversion, especially at 19:00 BT on 4 December reached maximum of 7°C/100 m. Moreover, the temperature did not decrease above the inversion layer; there was a 100 m thick layer of high temperature, so it was difficult for the thermal inversion layer to disappear. At 07:00 BT and 19:00 BT on 8 December, multilayer inversion appeared, which made the fog vertical structure more stable. The ground-layer inversion was beneficial to the accumulation of moisture and pollutants near the surface, and the upper-layer inversion was not conductive to the upward diffusion of moisture and pollutants, which prevented the dissipation of polluted fog. In the morning of 9 December, with the invasion of cold air from the north, the inversion layer disappeared in the boundary layer, the fog disappeared, and the concentration of $PM_{2.5}$ decreased obviously. Thus, the long-term maintenance of the inversion layer was one of the important conditions for the formation and maintenance of the strongly polluted fog.

To further analyze the inversion structure in the boundary layer, Figure 8 shows the spatial and temporal profiles of wind barb, temperature, and humidity at Shenyang site from 07:00 BT on 1 December to 19:00 BT on 9 December. On 3 and 4 December, the temperature of the whole layer rose due to the effects of southerly and easterly airflows, and a high temperature center formed at 200–500 m, whose center value was over 10°C, about 8°C higher than the ground temperature. The warm advection not only transported warm air but also brought in plenty of moisture.

Figure 9 shows time-height cross section of divergence. When the fog occurred, the divergence was positive below 925 hPa, and the divergence center was less than $2 \times 10^{-5} \cdot s^{-1}$. Figure 9 indicates that there was a downdraft in the middle and lower layers, which not only helped to form the inversion, but also transported moisture from the upper layer to the near-surface layer, and the air pollutants could not diffuse upward.

The above results show that strong thermal inversion layer was an important cause for the formation of the heavily polluted fog. The formation of the ground-layer inversion resulted from radiative cooling, while the warm advection above the inversion layer and downdraft were beneficial to the enhancement of the inversion layer.

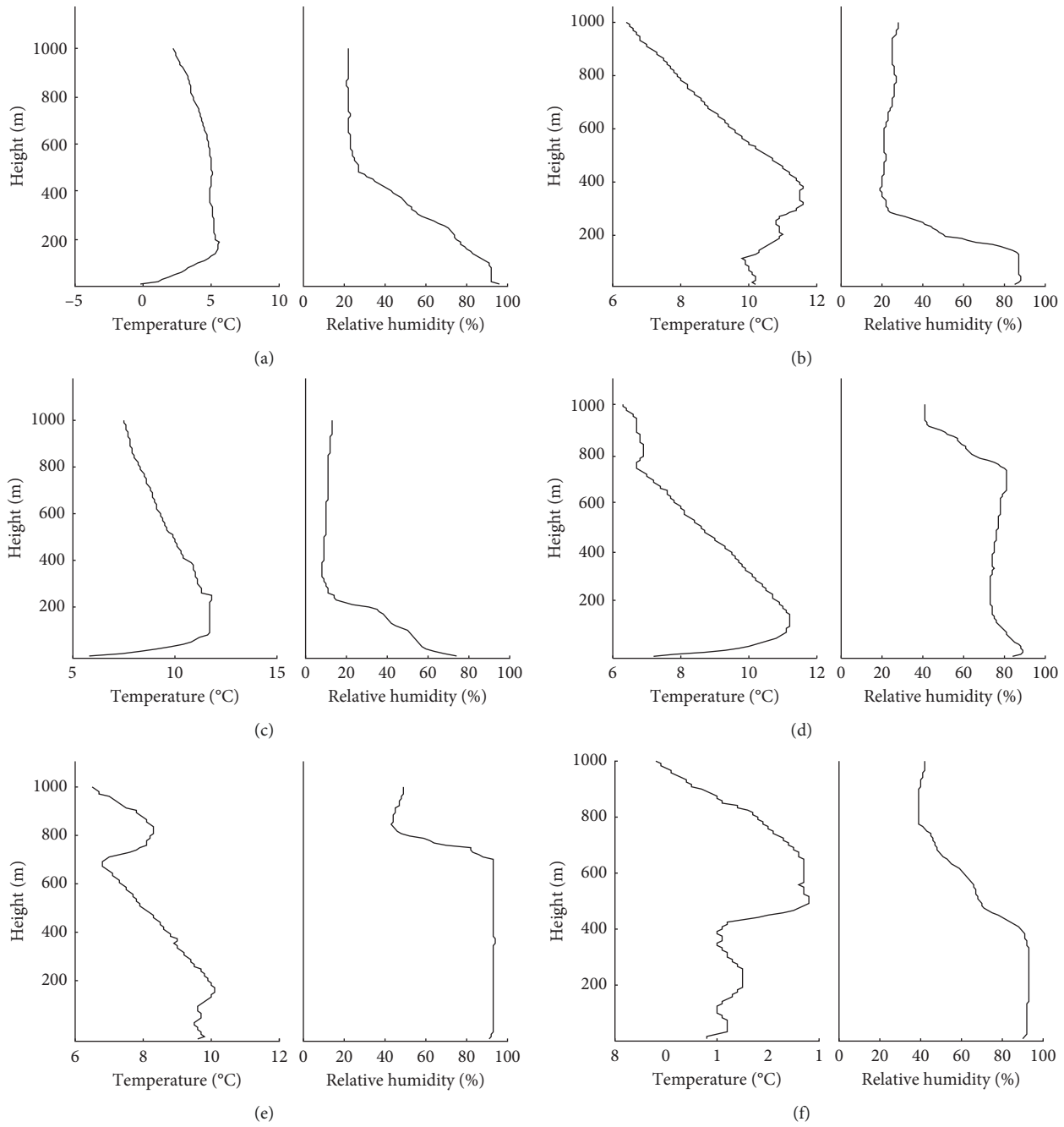

Figure 7: Vertical profiles of temperature and relative humidity at the Sheyang site from 1 to 9 December 2013: (a) 07:00 BT on 2 December, (b) 19:00 BT on 3 December, (c) 19:00 BT on 4 December, (d) 19:00 BT on 5 December, (e) 07:00 BT on 8 December, and (f) 19:00 BT on 8 December.

6. Causes for the Explosive Development of Severe Fog

Earlier, we pointed out that the five extremely dense fog processes all displayed explosive enhancement feature. So, what caused such explosiveness? Pu et al. [18, 19] noted that the longwave radiation enhancement at night and the sharp drop of temperature can lead to explosive enhancement; after sunrise, evaporation from the wet surface and cold advection near the surface layer make fog suddenly concentrated; the upper-layer warm advection, cold surface advection, and turbulent mixing can also lead to fog's explosive development. Four explosive fog processes happened during clear night, except for the last one, which was a frontal fog (Figure 10). The radiative cooling was one of the important factors, and the explosive development of fog resulted from accelerated cooling. At the same time, the wind direction suddenly turned to northwesterly, which indicated weak cold air invasion. As shown in Figure 2, in the evening of 4 December, it was clear sky at the Sheyang site with breeze and ground radiative cooling, and the temperature continued to fall by about 7°C from 17:00 BT to

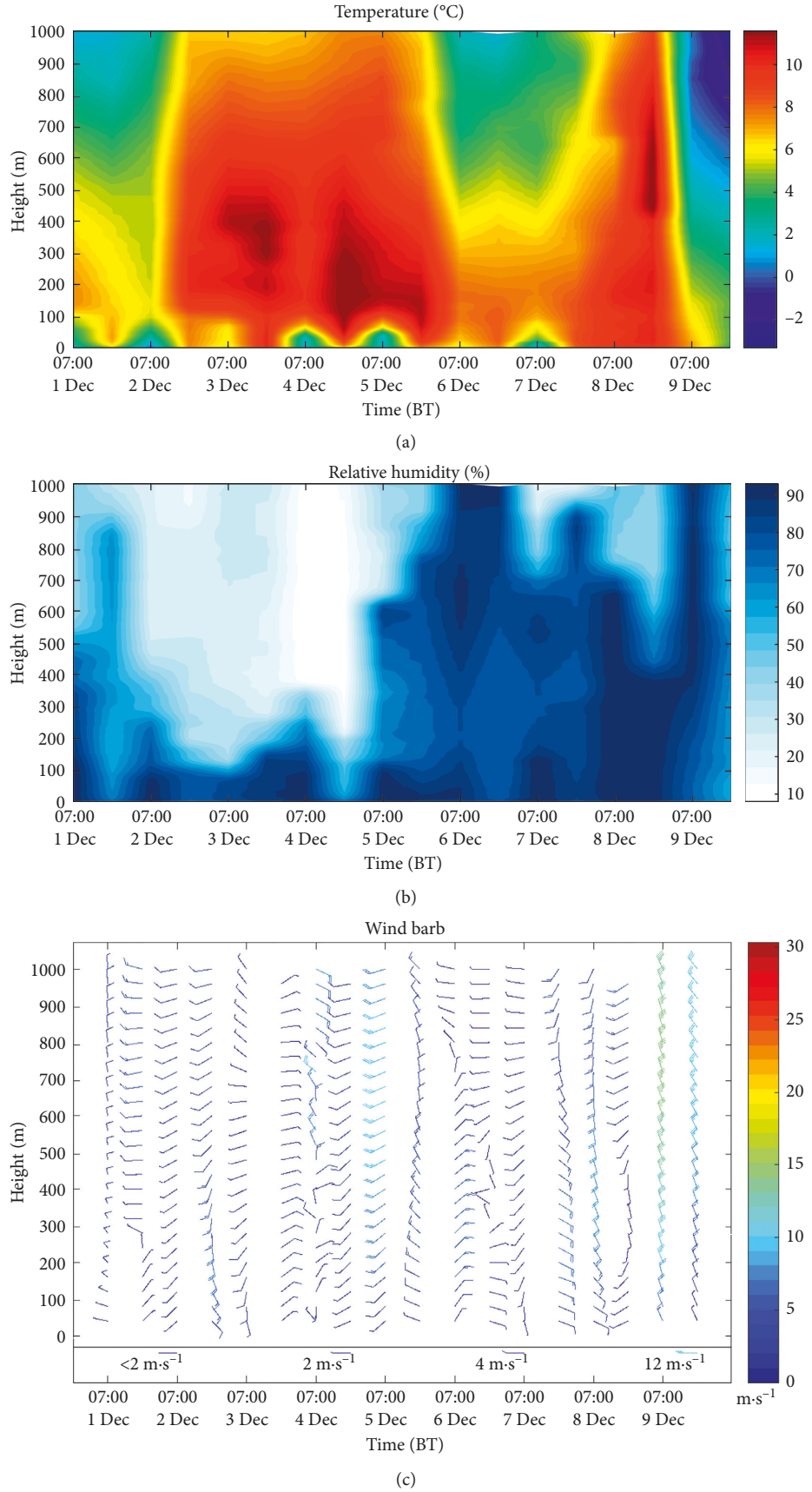

Figure 8: Time-height profile of (a) temperature, (b) relative humidity, and (c) wind barb at the Sheyang site from 07:00 BT on 1 December to 19:00 BT on 9 December 2013.

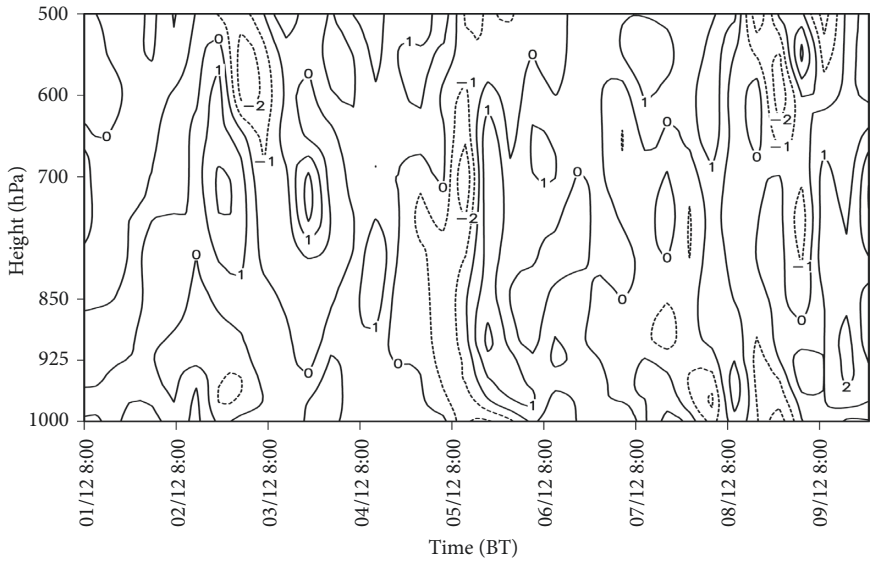

Figure 9: Time-height profile of divergence at the Sheyang site from 1 to 9 December 2013. Unit: $10^{-5}\cdot s^{-1}$.

20:00 BT; then, the fog formed. Since then, due to the latent heat release, the temperature rebounded slightly, and then both temperature and visibility dropped sharply. On 4 December, the visibility was 0.537 km at 23:52 BT, but it dropped to 0.027 km suddenly at 00:20 BT on 5 December, and the fog enhanced explosively. The sharp drop in temperature was due to radiative cooling and the wind direction changed to the northwesterly at the midnight of 00:00 BT, leading to the explosive enhancement. We can see that the explosive enhancement was related to weak cold air invasion. The severe fog that occurred in the morning of 7 December also explosively enhanced after the wind direction turned to westerly. The visibility at 00:36 BT was 1.772 km, but it dropped to 0.085 km quickly at 01:04 BT. It developed into severe fog in less than 30 min. Similarly, the explosive enhancement which occurred at 23:11 BT on 3 December was also related to the change of wind direction and sharp drop of temperature (Figure 2). The difference was that the weak precipitation started at 20:00 BT on 3 December, the cloud dissipated when the fog started, and the early precipitation increased surface humidity, which contributed to the fog enhancement. The continuous variation of fog droplet spectrum observations show that the burst broadening of fog droplet spectrum actually occurs under the condition of enhanced saturation which proceeds microphysical processes (e.g., condensation, collision, deposition, and nucleation) quickly. Therefore, the droplet concentration increases by about one order of magnitude. The spectral width of fog droplet spectrum exceeds 20 μm and can generally reaches 30–40 μm or even 50 μm. As a result, the LWC increases significantly (generally by two to three orders of magnitude). Thus, the visibility decreases to less than 0.05 km; that is, dense fog changes rapidly to extremely dense fog [18, 19].

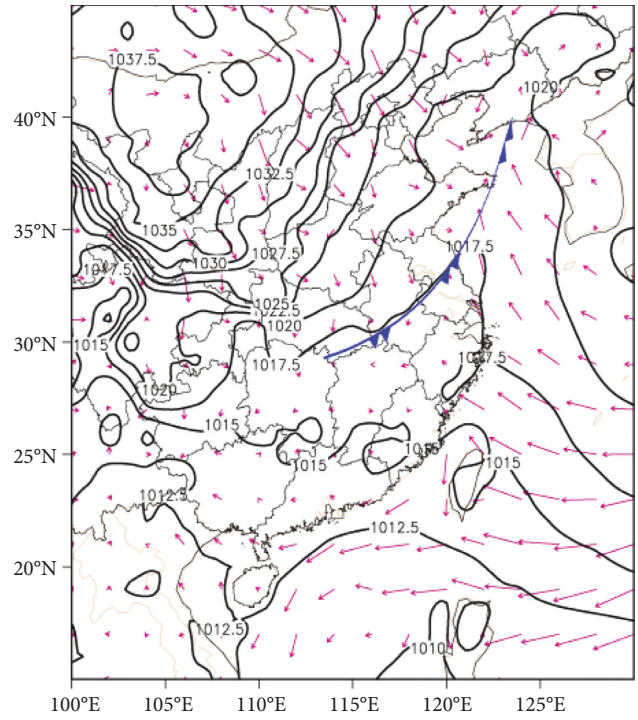

Figure 10: Surface fields: wind, sea-level pressure, and cold front at 20:00 BT on 8 December 2013.

7. Conclusions

In the early December 2013, a dense fog with heavily polluted air lasted for nine days in Yancheng, Jiangsu Province, China. Comprehensive analyses on the event were conducted in this study. The conclusions are as follows:

(1) The fog process was characterized by long duration and strong intensity. The $PM_{2.5}$ concentration increased obviously when severe fog occurred (except for the fog after the rain); that is, strong dense fog and heavy pollution appeared together. The fog was not transformed from haze. Only the polluted gases

(SO_2 and NO_2) exhibited obvious decline when absorbed by fog water.

(2) Atmospheric circulation contributed to the development and maintenance of heavily polluted fog. The existing southerly anomaly in the lower troposphere brought more moisture to the Jiangsu area, which provided moisture condition for fog formation. Meanwhile, the weakening of East Asian winter monsoon led to the weakening of surface wind, which favored fog formation and pollutants' accumulation, but not for transporting fog and pollutants outward via advection, resulting in the maintenance of the polluted fog process. The higher pressure in the middle troposphere controlled the development of convection and helped the polluted fog aggregated in the lower layer of the atmosphere. The decreasing vertical gradient of horizontal wind in the middle and lower troposphere not only suppressed the development of synoptic-scale disturbances by weakening the atmospheric baroclinic instability but also made the atmospheric stratification more stable by weakening vertical mixing.

(3) Under surface radiative cooling, sinking airflow in the lower level and warm, moist airflow from the south, a deep strong inversion of temperature layer was formed, which was the most important thermodynamic condition for the formation of these strong dense fogs, as well an important cause for the heavily polluted air.

(4) The fog process was accompanied by many times of explosive enhancements. Those enhancements happened almost within 30 min, and the shortest one was only 8 min with visibility dropping quickly from 1.29 km to 0.071 km, which was quite rare in previous observations. Weak cold air invasion and radiative cooling were the triggering factors for the explosiveness.

Conflicts of Interest

The authors declare that they have no conflicts of interest.

Acknowledgments

This work was jointly supported by the National Natural Science Foundation of China (Grant no. 41575135), the Natural Science Foundation of Jiangsu Province (Grant nos. BK20161073 and BE2016810), and the Beijige Foundation (Grant nos. BJG201503 and BJG201505).

References

[1] I. Gultepe, R. Tardif, S. C. Michaelides et al., "Fog research: a review of past achievements and future perspectives," *Pure and Applied Geophysics*, vol. 164, no. 6-7, pp. 1121–1159, 2007.

[2] J. Li, J. Sun, M. Zhou et al., "Observational analyses of dramatic developments of a severe air pollution event in the Beijing area," *Atmospheric Chemistry and Physics*, vol. 18, no. 6, pp. 3919–3935, 2018.

[3] J. Bartok, A. Bott, and M. Gera, "Fog prediction for road traffic safety in a coastal desert region," *Boundary-Layer Meteorology*, vol. 145, no. 3, pp. 485–506, 2012.

[4] G. Fu, P. Li, J. G. Crompton et al., "An observational and modeling study of a sea fog event over the Yellow Sea on 1 August 2003," *Meteorology and Atmospheric Physics*, vol. 107, no. 3-4, pp. 149–159, 2010.

[5] H. Tanaka, S. Honma, M. Nishi et al., "Acid fog and hospital visits for asthma: an epidemiological study," *European Respiratory Journal*, vol. 11, no. 6, pp. 1301–1306, 1998.

[6] C. Román-Cascón, C. Yague, M. Sastre et al., "Estimating fog-top height through near-surface micrometeorological measurements," *Atmospheric Research*, vol. 170, pp. 76–86, 2016.

[7] J. Cuxart, C. Yagüe, G. Morales et al., "Stable atmospheric boundary-layer experiment in Spain (SABLES 98): a report," *Boundary-Layer Meteorology*, vol. 96, no. 3, pp. 337–370, 2000.

[8] R. Tardif, "The impact of vertical resolution in the explicit numerical forecasting of radiation fog: a case study," *Pure and Applied Geophysics*, vol. 164, no. 6-7, pp. 1221–1240, 2007.

[9] S. Rémy and T. Bergot, "Assessing the impact of observations on a local numerical fog prediction system," *Quarterly Journal of the Royal Meteorological Society*, vol. 135, no. 642, pp. 1248–1265, 2009.

[10] D. Liu, J. Yang, S. Niu, and Z. Li, "On the evolution and structure of a radiation fog event in Nanjing," *Advances in Atmospheric Sciences*, vol. 28, no. 1, pp. 223–237, 2011.

[11] Z. Li, J. Huang, B. Sun et al., "Burst characteristics during the development of radiation fog," *Chinese Journal of Atmospheric Science*, vol. 23, no. 5, pp. 623–631, 1999, in Chinese.

[12] Z. Li, J. Huang, Y. Zhou et al., "Physical structures of the five-day sustained fog around Nanjing in 1996," *Acta Meteorologica Sinica*, vol. 57, no. 5, pp. 622–631, 1999, in Chinese.

[13] S. Niu, C. Lu, H. Yu, L. Zhao, and J. Lü, "Fog research in China: an overview," *Advances in Atmospheric Sciences*, vol. 27, no. 3, pp. 639–663, 2010.

[14] Q. Fan, A. Wang, S. Fan et al., "Numerical prediction experiment of an advection fog in Nanling mountain area," *Journal of Meteorological Research*, vol. 17, no. 3, pp. 337–349, 2003.

[15] S. Gao, H. Lin, B. Shen, and G. Fu, "A heavy sea fog event over the Yellow Sea in March 2005: analysis and numerical modeling," *Advances in Atmospheric Sciences*, vol. 24, no. 1, pp. 65–81, 2007.

[16] Z. Li, J. Huang, Y. Huang et al., "Study on the physical process of winter valley fog in Xishuangbanna Region," *Journal of Meteorological Research*, vol. 13, no. 4, pp. 494–508, 1999.

[17] L. Wang, S. Chen, and A. Dong, "The distribution and seasonal variations of fog in China," *Acta Geographica Sinica*, vol. 60, no. 4, pp. 134–139, 2005, in Chinese.

[18] M. Pu, G. Zhang, W. Yan et al., "Features of a rare advection-radiation fog event," *Science in China Series D-Earth Sciences*, vol. 38, no. 6, pp. 776–783, 2008, in Chinese.

[19] M. Pu, W. Yan, Z. Shang et al., "Study on the physical characteristics of burst reinforcement during the winter fog of Nanjing," *Plateau Meteorology*, vol. 27, no. 5, pp. 1111–1118, 2008, in Chinese.

[20] D. Liu, W. Yan, J. Yang, M. Pu, S. Niu, and Z. Li, "A study of the physical processes of an advection fog boundary layer," *Boundary-Layer Meteorology*, vol. 158, no. 1, pp. 125–138, 2016.

[21] C. Ma, B. Wu, Y. Li et al., "Mechanisms of formation and maintenance of 12-day long-drawn fog in central and southern Hebei Province," *Plateau Meteorology*, vol. 31, no. 6, pp. 1663–1674, 2012, in Chinese.

[22] D. Liu, M. Pu, J. Yang et al., "Microphysical structure and evolution of a four-day persistent fog event in Nanjing in December 2006," *Aerosol and Air Quality Research*, vol. 24, no. 1, pp. 104–115, 2010.

[23] D. Liu, Z. Li, W. Yan, and Y. Li, "Advances in fog microphysics research in China," *Asia-Pacific Journal of Atmospheric Sciences*, vol. 53, no. 1, pp. 1–18, 2017.

[24] Z. Li, J. Yang, C. Shi, and M. Pu, "Urbanization effects on fog in china: field research and modeling," *Pure and Applied Geophysics*, vol. 169, no. 5-6, pp. 927–939, 2012.

[25] J. L. Collett, D. E. Sherman, K. F. Moore, M. P. Hannigan, and T. Lee, "Aerosol particle processing and removal by fogs: observations in chemically heterogeneous central California radiation fogs," *Water Air and Soil Pollution Focus*, vol. 1, no. 5-6, pp. 303–312, 2001.

[26] I. Gultepe, M. D. Muller, and Z. Boybeyi, "A new visibility parameterization for warm-fog applications in numerical weather prediction models," *Journal of Applied Meteorology and Climatology*, vol. 45, no. 11, pp. 1469–1480, 2006.

[27] I. Gultepe and J. A. Milbrandt, "Microphysical observations and mesoscale model simulation of a warm fog case during FRAM project," *Pure and Applied Geophysics*, vol. 164, no. 6-7, pp. 1161–1178, 2007.

[28] I. Gultepe, G. Pearson, J. A. Milbrandt et al., "The fog remote sensing and modeling field project," *Bulletin of the American Meteorological Society*, vol. 90, no. 3, pp. 341–359, 2010.

[29] M. Haeffelin, T. Bergot, T. Elias et al., "Parisfog: shedding new light on fog physical processes," *Bulletin of the American Meteorological Society*, vol. 91, no. 6, pp. 767–783, 2010.

[30] R. G. Eldridge, "A few fog drop-size distributions," *Journal of Meteorology*, vol. 18, no. 5, pp. 671–676, 1961.

[31] R. G. Eldridge, "Haze and fog aerosol distributions," *Journal of the Atmospheric Sciences*, vol. 23, no. 5, pp. 605–613, 1966.

[32] R. G. Eldridge, "The relationship between visibility and liquid water content in fog," *Journal of the Atmospheric Sciences*, vol. 28, no. 7, pp. 1183–1186, 1971.

[33] J. Goodman, "The microstructure of California coastal fog and stratus," *Journal of Applied Meteorology*, vol. 16, no. 10, pp. 1056–1067, 1977.

[34] K. E. Pickering and J. E. Jiusto, "Observations of the relationship between dew and radiation fog," *Journal of Geophysical Research Oceans*, vol. 83, no. C5, pp. 2430–2436, 1978.

[35] H. Gerber, "Supersaturation and droplet spectral evolution in fog," *Journal of the Atmospheric Sciences*, vol. 48, no. 24, pp. 2569–2588, 1991.

[36] T. W. Choularton, G. Fullarton, J. Latham, C. S. Mill, M. H. Smith, and I. M. Stromberg, "A field study of radiation fog in Meppen, West Germany," *Quarterly Journal of the Royal Meteorological Society*, vol. 107, no. 452, pp. 381–394, 1981.

[37] M. Mohan and S. Payra, "Influence of aerosol spectrum and air pollutants on fog formation in urban environment of megacity Delhi, India," *Environmental Monitoring and Assessment*, vol. 151, no. 1-4, pp. 265–277, 2009.

[38] S. N. Pandis, C. Pilinis, and J. H. Seinfeld, "The smog-fog-smog cycle and acid deposition," *Journal of Geophysical Research Atmospheres*, vol. 95, no. 11, pp. 18489–18500, 1990.

[39] D. J. Jacob, J. M. Waldman, J. W. Munger, and M. R. Hoffmann, "A field investigation of physical and chemical mechanisms affecting pollutant concentrations in fog droplets," *Tellus Series B-Chemical and Physical Meteorology*, vol. 36, no. 4, pp. 272–285, 1984.

[40] H. Köhler, "The nucleus in and the growth of hygroscopic droplets," *Transactions of the Faraday Society*, vol. 32, pp. 1152–1161, 1936.

[41] C. Shi, X. Deng, B. Zhu et al., "Physical and chemical characteristics of atmospheric aerosol under the different weather conditions in Hefei," *Acta Meteorologica Sinica*, vol. 74, no. 1, pp. 149–163, 2016, in Chinese.

[42] China Meteorological Administration, *Grade of Fog Forecast*, The State Standard of the People's Republic of China, GB/T 27964 -2011, Beijing, China, 2011, in Chinese.

[43] China Meteorological Administration, *Observation and Forecasting Levels of Haze*, China Meteorological Press, Beijing, China, 2010, in Chinese.

[44] D. Liu, M. Pu, W. Yan et al., "Study on the formation and the cause of the fog-haze transformation in the lover reaches of Huaihe River," *China Environmental Science*, vol. 34, no. 7, pp. 1673–1683, 2014, in Chinese.

[45] D. Liu, X. Liu, H. Wang et al., "A new type of haze? The December 2015 purple (magenta) haze event in Nanjing, China," *Atmosphere*, vol. 8, no. 12, p. 76, 2017.

[46] Q. Jiang, Y. Sun, Z. Wang, and Y. Yin, "Aerosol composition and sources during the Chinese Spring Festival: fireworks, secondary aerosol, and holiday effects," *Atmospheric Chemistry and Physics*, vol. 15, no. 11, pp. 6023–6034, 2015.

[47] M. C. Barth, D. A. Hegg, and P. V. Hobbs, "Numerical modeling of cloud and precipitation chemistry associated with two rainbands and some comparisons with observations," *Journal of Geophysical Research Atmospheres*, vol. 97, no. D5, pp. 5825–5845, 1992.

[48] Q. Zhang, X. Tie, W. Lin et al., "Variability of SO_2 in an intensive fog in North China Plain: evidence of high solubility SO_2," *Particuology*, vol. 11, no. 1, pp. 41–47, 2013.

[49] W. Birmili and A. Wiedensohler, "New particles formation in the continental boundary layer: meteorological and gas phase parameter influence," *Geophysical Research Letters*, vol. 27, no. 20, pp. 3325–3328, 2000.

[50] J. Du, T. Cheng, M. Zhang et al., "Aerosol size spectra and particle formation events at urban Shanghai in eastern China," *Aerosol and Air Quality Research*, vol. 12, no. 6, pp. 1362–1372, 2012.

[51] H. Guo, D. Wang, K. Cheung, Z. H. Ling, C. K. Chan, and X. H. Yao, "Observation of aerosol size distribution and new particle formation at a mountain site in subtropical Hong Kong," *Atmospheric Chemistry and Physics*, vol. 12, no. 20, pp. 9923–9939, 2012.